Vol.4, No.5, 313-323 (2012)
http://dx.doi.org/10.4236/ns.2012.45044

Natural Science

The diffusion and concentration effects of formamide on a TiO_2 surface in the presence of a water solvent

Ermuhammad Dushanov[1,2], Kholmirzo Kholmurodov[1,3*], Kenji Yasuoka[4]

[1]Laboratory of Radiation Biology, Joint Institute for Nuclear Research, Dubna, Russia; [*]Corresponding Author: mirzo@jinr.ru
[2]Institute of Nuclear Physics, Tashkent, Uzbekistan
[3]Dubna International University, Moscow, Russia
[4]Department of Mechanical Engineering, Keio University, Yokohama, Japan

Received 22 February 2012; revised 20 March 2012; accepted 3 April 2012

ABSTRACT

The formamide-titanium oxide interaction mechanism is a research target of great importance for understanding the elementary events of the origin of life: the synthesis of nucleoside bases and formation of biological molecules needed for life. Titanium oxide (TiO_2) can act as a strongly adsorbing surface or a catalytic material. In the present study, a comparative molecular dynamics analysis performed to clarify the adsorbing and diffusion properties of liquid formamide on a TiO_2 surface in the presence of water molecules. The structural features of the formamide concentration effect (the accumulation of molecules) on a TiO_2 surface in the presence and absence of water solvent are cleared up. Modification of the formamide diffusion abilities mediated by a water solvent is observed to correlate with the formamide-water concentration distribution on the surface.

Keywords: Molecular Dynamics Simulations; Formamide Molecule; Water Solvent; Diffusion Coefficient; Anatase Surface; RDF Graphs

1. INTRODUCTION

The photoreaction of liquid formamide on titanium oxide is widely considered to be one of the key steps in the formation of biological molecules needed for life. The titanium oxide (TiO_2) surface can act both as a template on which the accumulation of adsorbed molecules occurs (the concentration effect), and a catalytic material that lowers the activation energy needed for the formation of intermediate products [1-5]. The solvent, dehydration, adsorption, and decomposition properties of formamide on various surfaces were intensively studied in recent experimental papers [6-8]. In surface chemistry, titanium dioxide (TiO_2) is one of the most innovative materials. In this regard, the water-TiO_2 interaction is a special research target both in materials and life sciences, taking into account the wide range of technological applications of the phenomena. The mechanism of the interaction between water and oxide materials has long been studied in a wide variety of fundamental scientific disciplines [9]. Understanding the water-surface interaction mechanism is critically important for chemical and pharmaceutical industries, as well as for the fabrication of new materials and drugs [10-14]. Much of the research in surface chemistry that is focused on the water-TiO_2 interaction has been motivated by the relatively high efficiency of TiO_2 in the photocatalytic decomposition of water. The water-TiO_2 interaction is potentially important as a solar energy conversion process. The photocatalytic properties of these materials in aqueous media have been studied since mid-1970's [11]. These studies have inspired, in particular, work on well-characterized single crystals of oxides. From the biological point of view, the TiO_2 surfaces have been of the most interest concerning the photochemical degradation of organic compounds such as bactericides and hydrophobic coatings [13]. The TiO_2-water reactions seem to be very promising in the field of solar energy conversion by means of the photocatalytic splitting of water (the Fujishima-Honda reaction in [14]).

Formamide (the molecular formula: CH_3NO), also known as methanamide, is an amide derived from formic acid. It is a clear liquid which is miscible with water and has an ammonia-like odor. When heated strongly, formamide decomposes to hydrogen cyanide (HCN) and water vapor. As a constituent part, formamide is also used for the cryopreservation of tissues and organs. In relation to the DNA and RNA molecules, some important formamide's properties could be outlined as follows. It stabilizes RNA in gel electrophoresis by deionizing RNA; in capillary electrophoresis, it is used for stabilizing single

strands of denatured DNA. Formamide lowers the melting point of nucleic acids so that the strands separate more readily [15].

An important type of nucleoside bases synthesis can be supposed to take place under UV light in the formamide reaction with a TiO_2 surface, which would underlie the crucial biological significance of this mineral in making compounds of life. In the dark conditions, the experimental data on the formamide adsorption at 300 K over TiO_2 (001) indicate some amount of unreacted formamide and water among the products (CO, H_2, NH_3, HCN). Thus, some concentration of water and its involvement in the formamide-TiO_2 interaction was experimentally shown to be a constituent and important factor. Besides of nucleoside synthesis, formamide actively influences *in situ* hybridization processes of the nucleotides, DNA and RNA molecules. For example, in the presence of formamide, a U nucleotide would rather bind to an A than nothing (binding to a specific probe is better than staying single-stranded), but a U nucleotide would rather bind to nothing than a G (binding to a non-specific probe is worse than binding to nothing). In this respect, DNA is normally more stable in a double-stranded structure and less stable when single-stranded; so far, formamide must increase the stability of single-strandedness. On other hand, RNA probe binds to mRNA that is already single-stranded; mRNA does not gain any stability by being a hybrid unless the probe is specific and can bind properly, thus increasing stability [1-5,15-17].

Apart from experimental research, recent theoretical and simulation studies were mostly concentrated on the formamide-water reaction process. Several modern theoretical and molecular dynamics (MD) studies of formamide-water interactions should be mentioned in this respect [18,19]. Nevertheless, to our best knowledge, little is known about the formamide-TiO_2 surface interaction, and almost nothing has been reported on the formamide-water-TiO_2 one. In this paper, using the MD simulation method, we aimed to make the first attempts to investigate the formamide-TiO_2 surface interaction mechanism in detail on the atomistic/molecular level. In the presence of water, we elucidate the structural, diffusional, and molecular concentration distribution effects. We consider water presence and influences to be a stabilizing factor on the formamide-TiO_2 surface interaction mechanism.

2. METHOD

A classical molecular dynamics study was performed using the DL_POLY 2.20 [20] general-purpose code. The NVT ensemble at T = 300 K in conjunction with a Nose-Hoover thermostat with the three-dimensional Ewald summation and the Verlet leapfrog scheme were employed. The integration time step of the dynamical equations of motion was 2 fs. All simulations were periodic in three dimensions.

For the formamide molecule, the force field parameters were chosen from the DL_FIELD database [21], which, in their turn, had been taken from the CHARMM package [22].

The detailed formamide potential topology (chemical bonds, angular and dihedral parameters, atomic charges, etc.) are described below in **Tables 1-3**.

Table 1. The Lennard-Jones (LJ) potential parameters for the formamide interactions with the TiO_2 surface and water molecules. The geometry of the formamide and water molecules are shown separately.

Group	ε, kcal·mol^{-1}	σ, Å
N-N	0.2000	3.2963
N-H1	0.0959	1.8482
N-H2	0.0959	1.8482
N-C	0.1183	3.4300
N-Hf	0.0663	2.8241
N-O	0.1549	3.1627
N-OW	0.1744	3.2234
N-Ti	0.7010	4.1310
C-C	0.0700	3.5636
C-H1	0.0567	1.9818
C-H2	0.0567	1.9818
C-O	0.0917	3.2963
C-OW	0.1032	3.3571
C-Ti	7.2630	4.1340
Of-Of	0.1200	3.0291
Of-H1	0.0743	1.7145
Of-H2	0.0743	1.7145
Of-Hf	0.0514	2.6905
Of-Ti	7.7253	2.3431
Of-O	0.2278	3.1306
Of-OW	0.2278	3.1306
Hf-Hf	0.0220	2.3520
Hf-H1	0.0318	1.3760
Hf-H2	0.0318	1.3760
Hf-OW	0.0578	2.7513
H1-H1	0.0460	0.4000
H1-H2	0.0460	0.4000
H1-OW	0.0836	1.7753
H1-HW	0.0460	0.4000
H2-H2	0.0460	0.4000
H2-OW	0.0836	1.7753
H2-HW	0.0460	0.4000

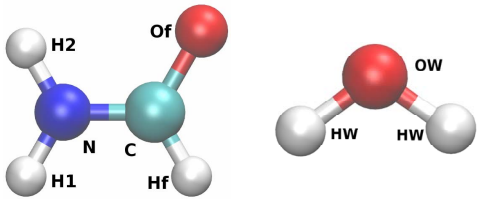

Table 2. The masses and effective partial charges of the formamide atoms in a.u.

Atom	m/m_e, a.m.u.	q/e, proton charge
1(N)	14.0067	–0.69
2(H1)	1.00797	+0.35
3(H2)	1.00797	+0.35
4(C)	12.0110	+0.42
5(Hf)	1.00797	+0.08
6(Of)	15.99940	–0.51

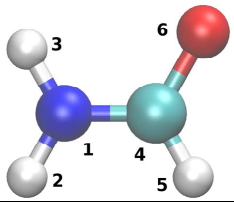

Table 3. The potential parameters used by formamide molecules.

	Harmonic bond potential: $K(r_{ij}-r_0)^2/2$	
Bond	K, kcal·mol^{-1}·Å	r_0, Å
N-H1	960.00	1.00
N-H2	960.00	1.00
N-C	860.00	1.36
C-Of	1300.00	1.23
C-Hf	634.26	1.10
N-Of	100.00	2.37
N-Hf	100.00	1.98
	12-6 potential bond: $A/r_{ij}^{12}-B/r_{ij}^6$	
Bond	A, kcal·mol^{-1}·Å^{12}	B, kcal·mol^{-1}·Å^6
H1-Of	25.09609	2.7310
H1-Hf	5.861992	0.8637
H2-Of	25.09609	2.7310
H2-Hf	5.861992	0.8637
	Angular potential: $K(\theta_{ijk}-\theta_0)^2/2$	
Group	K, kcal·mol^{-1}·rad^{-2}	θ_0, °
H1-N-H2	46.00	120.00
H1-N-C	100.00	120.00
H2-N-C	100.00	120.00
N-C-Of	150.00	122.00
N-C-Hf	88.00	111.00
Of-C-Hf	88.00	122.00
	Dihedral potential: $K[1+\cos(m\phi_{ijkn}-\delta)]$	
Group	K, kcal·mol^{-1}	δ, °	m
H1-N-C-Of	1.40	180	2
H1-N-C-Hf	1.40	180	2
H2-N-C-Of	1.40	180	2
H2-N-C-Hf	1.40	180	2

For the oxide materials, the force fields as reported by Kavathekar *et al*. [23] and Guillot *et al*. [24] were used. For the TiO_2 surface, the potential parameters were developed by Matsui and Akaogi [25]. **Table 4** represents the Buckingham (buck) potential parameters of the TiO_2 surface [25].

For water, an SPC rigid body model was used [26-28]. The water bond angles and lengths were not constrained; the water potential parameters are also shown in **Table 4**.

The van der Waals (vdW) interactions between the formamide + water solution and the oxide surface were represented by the Lennard-Jones (LJ) potential. The cross-interaction parameters for the formamide + water and TiO_2 surface are shown in **Tables 1** and **4**.

A parallel Shake algorithm expressed in terms of the Replicated Data strategy for constraining the rigid and other chemical bonds was used [20].

The MD simulations were realized in the temperature range from 250 K to 400 K with a step of 25 K.

For each simulation set, the MD calculations included 50,000 - 500,000 time steps of the integration of the equations of motion.

The LJ potential parameter in **Table 4** for the Ti-OW pair—compared with others—seems to be large: ε_{ij} = 7.72528 kcal/mol. Such a large ε_{ij} value for the Ti-OW pair was noted in other studies, too (see, for example, [29]). Nevertheless, our MD calculation results (as described below) exhibit a weaker or no dependence on the vdW interaction parameters of **Table 1**. For example, performing the test calculations with the following several values: ε_{ij} = 7.72528; 7.72528/10; 7.72528/100 kcal/mol —we got similar results. Moreover, all the vdW interaction parameters shown in **Tables 1** and **4** were slightly varied in their reasonable ranges; however, the final

Table 4. The force field potentials and parameters for a TiO_2 surface and a formamide + water solution.

Buckingham potential for TiO_2: $A_{ij}\exp(-r_{ij}/\rho_{ij})-C_{ij}/r_{ij}^6$			
$i-j$	A_{ij}, kcal·mol^{-1}	ρ, Å	C_{ij}, kcal·mol^{-1}·Å^6
Ti-Ti	717647.4	0.154	121.067
Ti-O	391049.1	0.194	290.331
O-O	271716.3	0.234	696.888
LJ potential for TiO_2, formamide and water: $q_iq_j/r_{ij}+\varepsilon_{ij}[(\sigma_{ij}/r_{ij})^{12}-(\sigma_{ij}/r_{ij})^6]$			
$i-j$	ε_{ij}, kcal·mol^{-1}		σ_{ij}, Å
Ti-OW	7.72528		2.3431
O-OW	0.22784		3.1306
OW-OW	0.15543		3.5532
HW-HW	0.04600		0.4000
Atomic charges: q(Ti) = 2.196e; q(O) = –1.098e; q(N) = –0.69e; q(C) = 0.42e; q(H1) = q(H2) = 0.35e; q(Of) = –0.51e; q(OW) = –0.82e; q(HW) = 0.41e			

results do not exhibit any substantial difference here. We also used other potential forms—different than the LJ and Buckingham ones—to describe the water-oxide surface interaction; however, the results obtained were similar to each other.

We have simulated various formamide and water-formamide mixtures (from low to high-density phases and of the 50% - 50% solution) in the range of ρ = [0.1 - 1.5] g/cm^3.

The MD simulation results of the formamide(f) + water(w) solution and surface interactions which are summarized below are shown for: (1) $\rho \approx 0.6$ g/cm^3 = 50%(f) + 50%(w) (170 formamide and 170 water molecules), (2) $\rho \approx 0.9$ g/cm^3 = 50%(f) + 50%(w) (256 formamide and 256 water molecules), and (3) $\rho \approx 1.3$ g/cm^3 = 50%(f) + 50%(w) (360 formamide and 360 water molecules).

The bulk TiO_2 (anatase) phase was defined by the unit cell lattice vectors of the following lengths: $a_0 = b_0$ = 3.785 Å, c_0 = 9.514 Å. As the adsorbing surface, we have composed in total four layers of 128 TiO_2 molecules (1536 = 512 (Ti) + 1024 (O) atoms).

The corresponding system sizes and molecular composition of 50% - 50% formamide-water solution for ρ = 0.6 g/cm^3; 0.9 g/cm^3; 1.3 g/cm^3 are specified in **Table 5**.

3. RESULTS AND DISCISSION

3.1. Surface-Liquid Ordering in the Formamide-Water-TiO_2 Interactions

Figure 1 shows a relaxed configuration of the molecular system (formamide molecules solvated by water on a TiO_2 surface). Two molecules (a formamide molecule and a water one) are denoted as large spherical balls; the surface Ti and O atoms—as green and red balls, respectively. The system temperature has been varied in the range of 250 - 400 K to ensure the structure stability of the oxide material in this temperature range; the oxide surface behaved stably, though the atoms of TiO_2 do not adopt a regular close-packing arrangement as thermal vibrations will slightly displace the surface atoms from their mean equilibrium positions. The oxide surface shown in the figure seems to be that of an amorphous solid.

First, based on the radial distribution functions (RDFs), we have investigated the structural peculiarities of TiO_2 during the relaxation process with the formamide-water

Table 5. The geometry details and molecular composition of the simulated models for a formamide(f)-water(w) solution and a TiO_2 surface.

System size	*X*, Å	*Y*, Å	*Z*, Å
$(TiO_2)_{1536}(H_2O)_{510}(CH_3NO)_{1020}$	30.28	30.28	51.692
$(TiO_2)_{1536}(H_2O)_{768}(CH_3NO)_{1536}$	30.28	30.28	51.692
$(TiO_2)_{1536}(H_2O)_{1080}(CH_3NO)_{2160}$	30.28	30.28	51.692

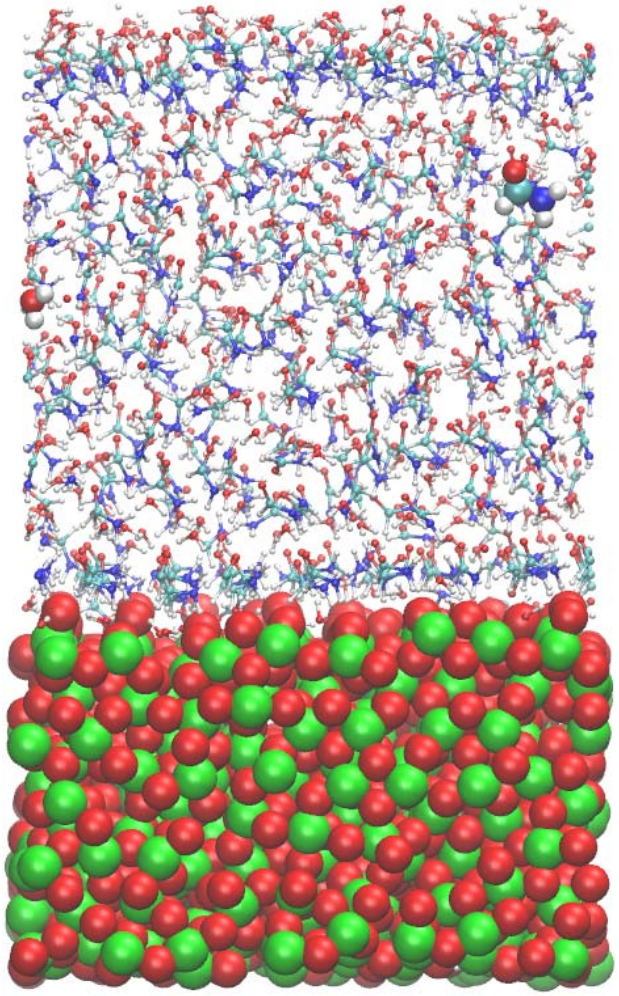

Figure 1. A snapshot of the formamide molecules solvated by water on a TiO_2 surface (Ti atoms—green, O atoms—red balls) is shown. Two molecules (one formamide and one water) are specified in larger scales.

mixture. In **Figures 2**, RDFs, $g(r)$, are presented for the final relaxed states of the oxide surface as follows: (left) at ρ = 0.6 g/cm^3, (middle) at ρ = 0.9 g/cm^3, and (right) at ρ = 1.3 g/cm^3 densities of the 50% - 50% formamide-water (f+w) solution. The RDFs presented in **Figure 2** show the surface-surface (Ti-Ti and Ti-O atomic pairs) and surface-water (Ti-OW pair) interaction ordering, respectively (from top to bottom: Ti-Ti, Ti-O, and Ti-OW).

For the surface-surface atomic pair $g(r)$ [Ti-O] with their opposite charges, we see that the Ti-O interaction is relatively very strong; such behavior agrees with the results reported in the literature earlier [30]. From **Figure 2**, we can also see that the interaction ordering of all atomic pairs (Ti-Ti, Ti-O, and Ti-OW) is more or less modified with changes in the density of the 50% - 50% formamide-water (f+w) solution. Comparing the structural RDF data in **Figure 2**, we will focus mostly on the middle density case, ρ = 0.9 g/cm^3. At low densities ($\rho \leq 0.6$ g/cm^3), we

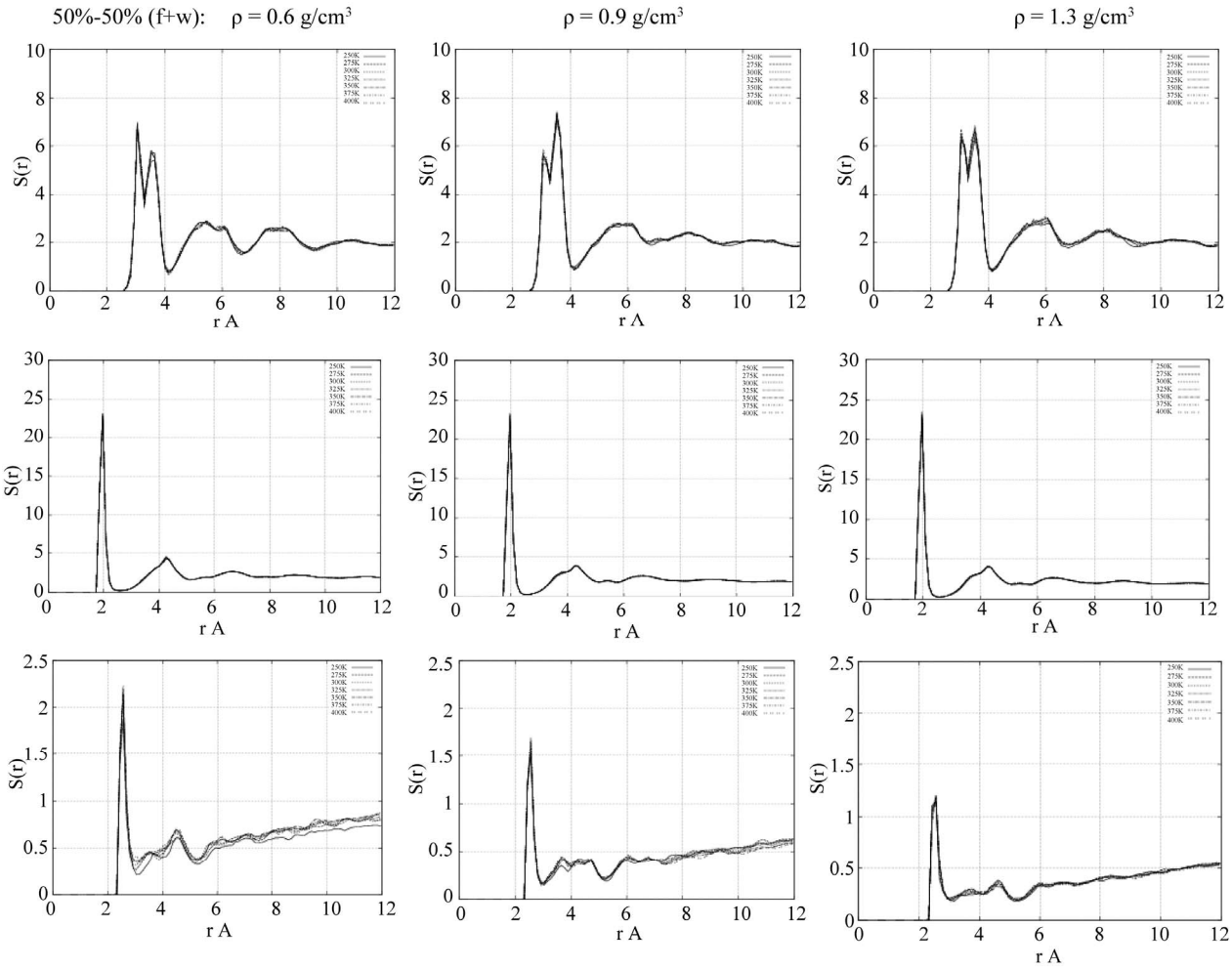

Figure 2. The radial distribution functions (RDFs) of the surface-surface and surface-water atomic pair interactions at the 50% - 50% formamide(f)-water(w) concentrations: (from left to right) ρ = 0.6 g/cm^3 = 50% - 50%(f + w); 0.9 g/cm^3 = 50% - 50%(f + w); and 1.3 g/cm^3 = 50% - 50%(f + w), respectively. Top: titan-titan (Ti-Ti); middle: titan-oxygen (Ti-O); bottom: titan-water's oxygen (Ti-OW) atomic pairs.

have a rather fast adsorption process for the solution on the surface; at high densities ($\rho \geq$ 1.3 g/cm^3), the formamide-water-surface system exhibits low adsorption activity. We will consider mainly the formamide-TiO_2 surface interaction, that is, the changes in the atomic pair ordering and diffusion processes, which are influenced by the presence of water.

In **Figure 3**, the RDFs are presented for the formamide ordering on a TiO_2 surface. The RDFs in **Figure 3** demonstrate the titan-formamide's oxygen interaction in the absence (top) and presence (bottom) of water. The inclusion of water, as it can be easily seen, makes the Ti-Of ordering rather smooth. Such behavior is observed in all the studied temperature range—from 250 up to 400 K.

3.2. Liquid-Liquid Ordering in the Formamide-Water-TiO_2 Interactions

The RDF-based liquid-liquid structural ordering is shown in **Figures 4**-**5** for the water-water (OW-OW) and formamide-formamide (Of-Of) atomic pair interactions, respectively. For the water-water interaction, we can observe from **Figure 4**, $g(r)$[OW-OW], that at low densities ($\rho \leq$ 0.6 g/cm^3) the RDFs visibly vary with temperature, while at high densities ($\rho \geq$ 1.3 g/cm^3) the RDFs are more structured and are not "sensitive" at all to temperature changes. At the studied moderate densities ($\rho \approx$ 0.9 g/cm^3), the $g(r)$[OW-OW] behaves like that of a liquid state, although compared to low and high densities, the RDFs have here the lowest peak amplitudes. Such structural behavior of water can be suggested to cause different formamide structure formation as well as diffusion processes on the TiO_2 oxide surface in the presence of water.

Figure 5 shows the RDFs $g(r)$[Of-Of] of the formamide-formamide atomic pair interactions in the absence and presence of water, respectively. One can expect that the

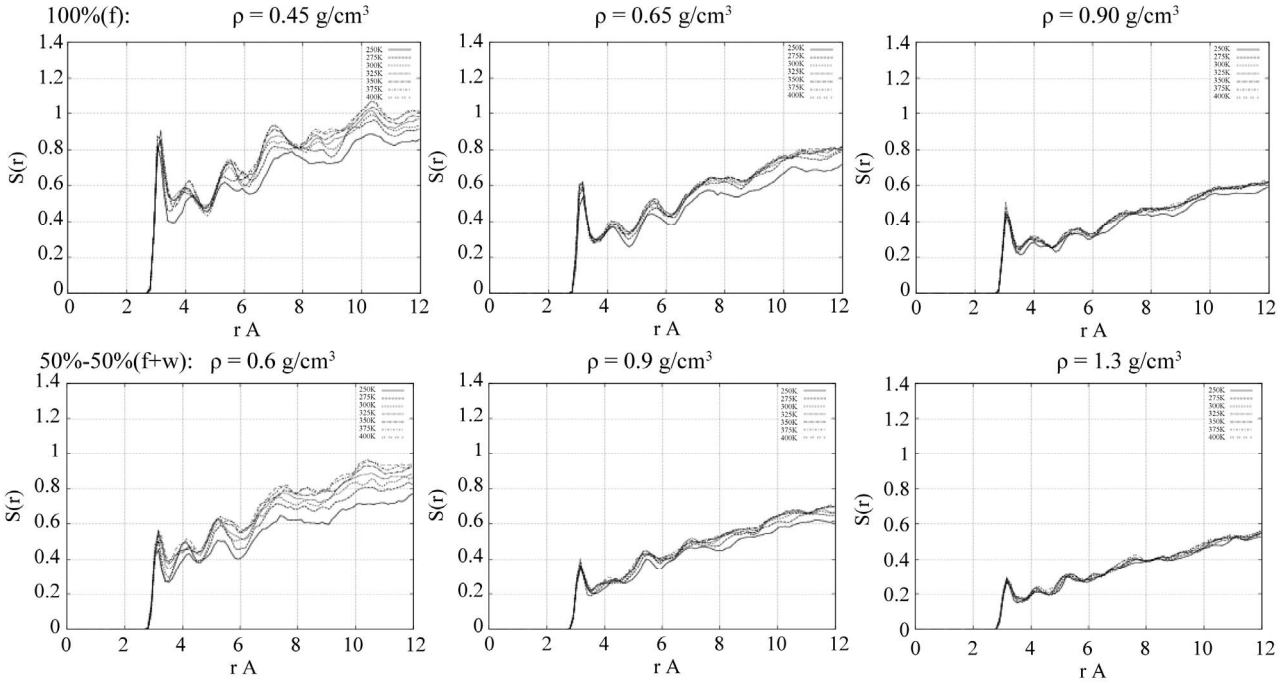

Figure 3. The radial distribution functions (RDFs) of the surface-liquid formamide atomic pair interactions at different 50% - 50% formamide(f)-water(w) concentration densities: (from left to right) $\rho = 0.6$ g/cm^3 = 50% - 50%(f + w); 0.9 g/cm^3 = 50% - 50%(f + w); and 1.3 g/cm^3 = 50% - 50%(f + w), respectively. Top: titan-formamide's oxygen (Ti-Of) in the absence of water; bottom: titan-formamide's oxygen (Ti-Of) in the presence of water.

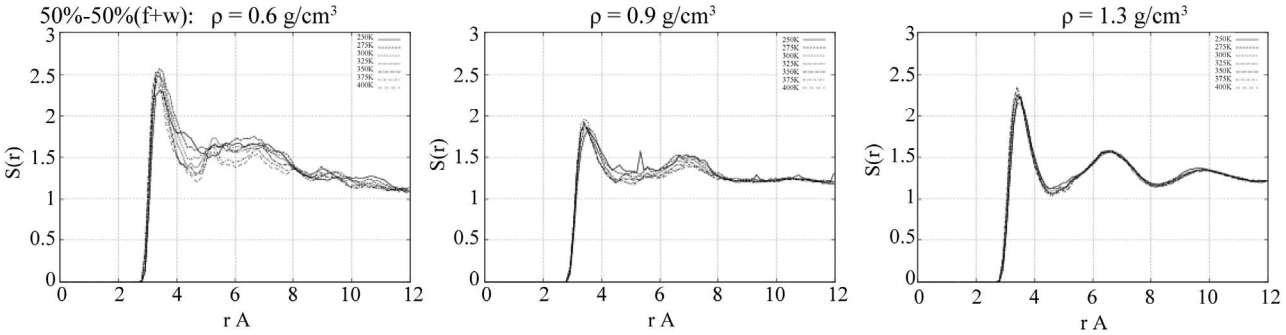

Figure 4. The radial distribution functions (RDFs) of the liquid-liquid atomic pair interactions: oxygen-oxygen (OW-OW) of the formamide-water mixture.

behavior of the RDFs is more clearly influenced by the presence of water mostly at moderate densities, $\rho \approx 0.9$ g/cm^3. In the absence of water (**Figure 5**, top middle picture), the first peak of the $g(r)$[Of-Of] is split into two very close maximums; this splitting disappears with the inclusion of water into consideration (**Figure 5**, bottom middle picture).

3.3. Z-Density Profiles and Diffusion Coefficients

In this section, based on the formamide-water-surface structure peculiarities described above, we discuss the Z-density profiles and the accumulation of formamide molecules on a TiO_2 surface (the formamide concentration effect) in correlation with the diffusion properties and $D(T)$ dependence. The concentration distributions in the molecular model under consideration are shown in **Figure 6**, where displayed are three sequential formamide-water surface configuration snapshots at different relaxation stages after the system has reached its equilibrium. MD simulation starts from equilibrium after sample minimization and heating steps have been completed; thus, all the statistical data are acquired in subsequent relaxed states.

In **Figure 7** (top graphs), plots of the density profiles of formamide molecules in the absence of water solvent are shown as a function of the perpendicular distance

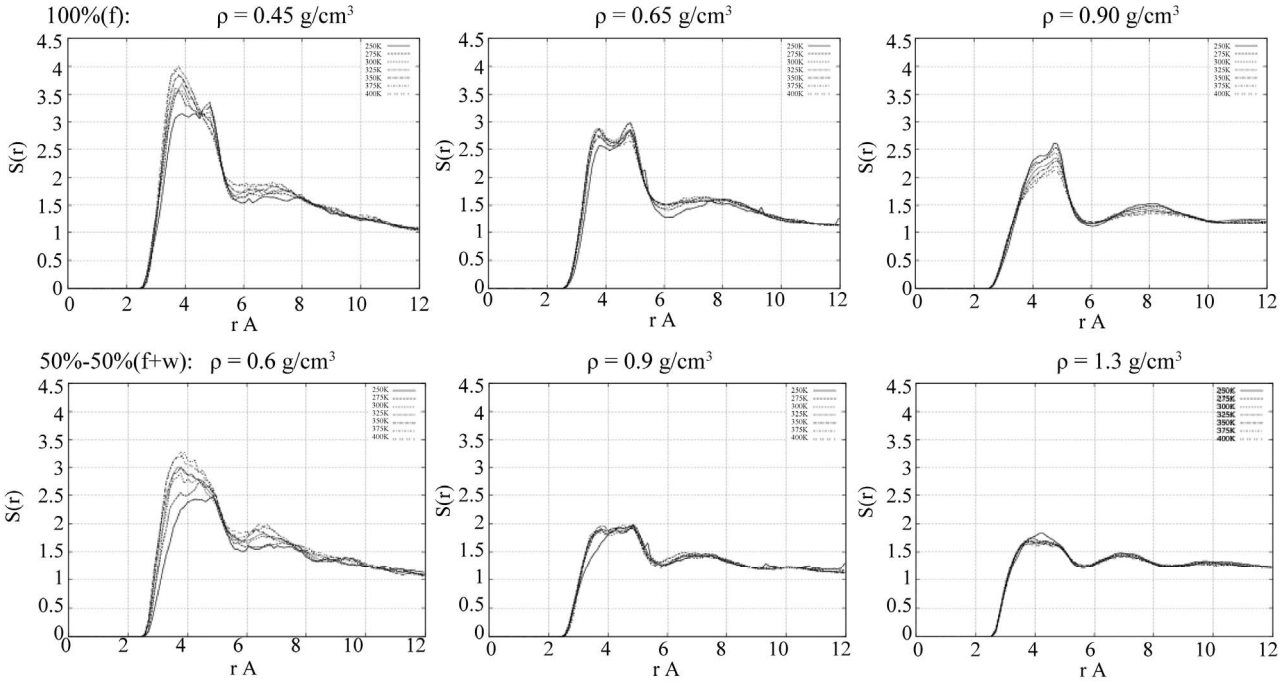

Figure 5. The radial distribution functions (RDFs) of the liquid-liquid atomic pair interactions. Top: oxygen-oxygen (Of-Of) in the absence of water; bottom: oxygen-oxygen (Of-Of) in the presence of water.

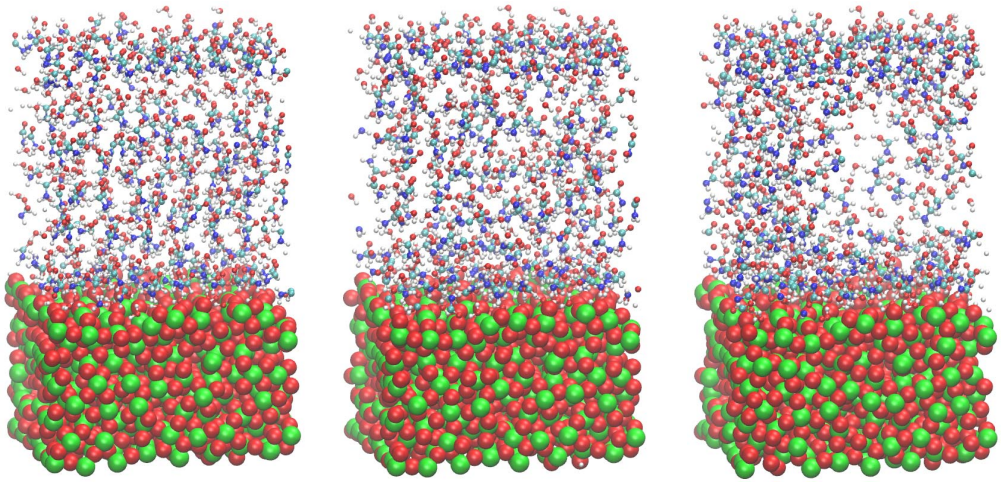

Figure 6. Three sequential snapshots of the surface-liquid formamide in the presence of water solvent at the initial (left; t = 0.0), intermediate (middle; t = 0.01 ns) and final (right; t = 1.0 ns) states.

from the TiO_2 surface. The densities were normalized relative to the bulk densities of the solution, which were ρ = 0.45 g/cm^3 = 100%(f + 0), 0.65 g/cm^3 = 100%(f + 0), and 0.9 g/cm^3 = 100%(f + 0), respectively. At a moderate density (middle graph), we observe the formation of two clear formamide concentration layers on the surface. The bottom graph of **Figure 7** illustrates the behavior of the formamide diffusion coefficient depending on temperature, $D(T)$. At low formamide concentrations, we observe a fast adsorption process, so the formamide diffusion ability decreases. It is also obvious that $D(T)$ correlates with the liquid concentration and increases with increasing the solution density.

Figure 8 (top graphs) show the Z-density profiles of water molecules of the 50% - 50% formamide-water (f + w) solution on a TiO_2 surface at low, moderate, and high densities as outlined above. Since the water molecule is small in size compared to the formamide one, the water Z-density profile at moderate (f + w) concentration exhibits more than two small peaks, indicating possibilities of the formation of multiple water layers inside formamide. As we see below, this fact is crucial and causes

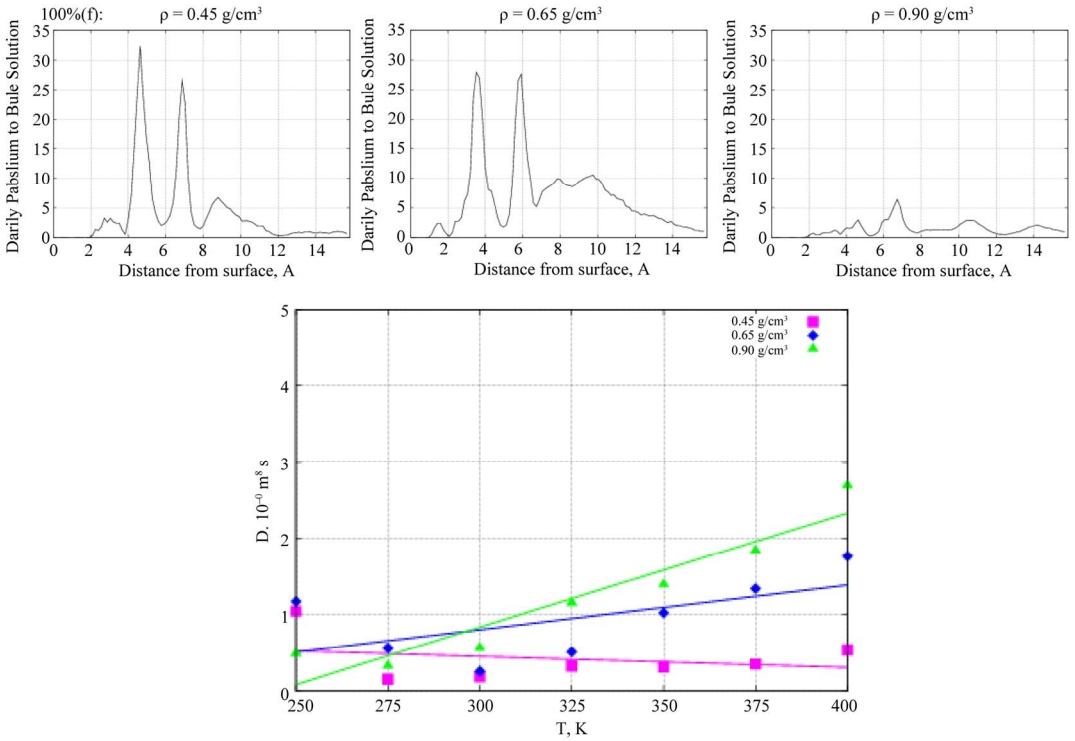

Figure 7. (top) The Z-density profiles of formamide molecules in the absence of water solvent are shown as a function of perpendicular distance from the TiO_2 surface. (bottom) $D(T)$ behavior of the formamide molecules vs liquid density (pink—low, blue—moderate, green—high density phases).

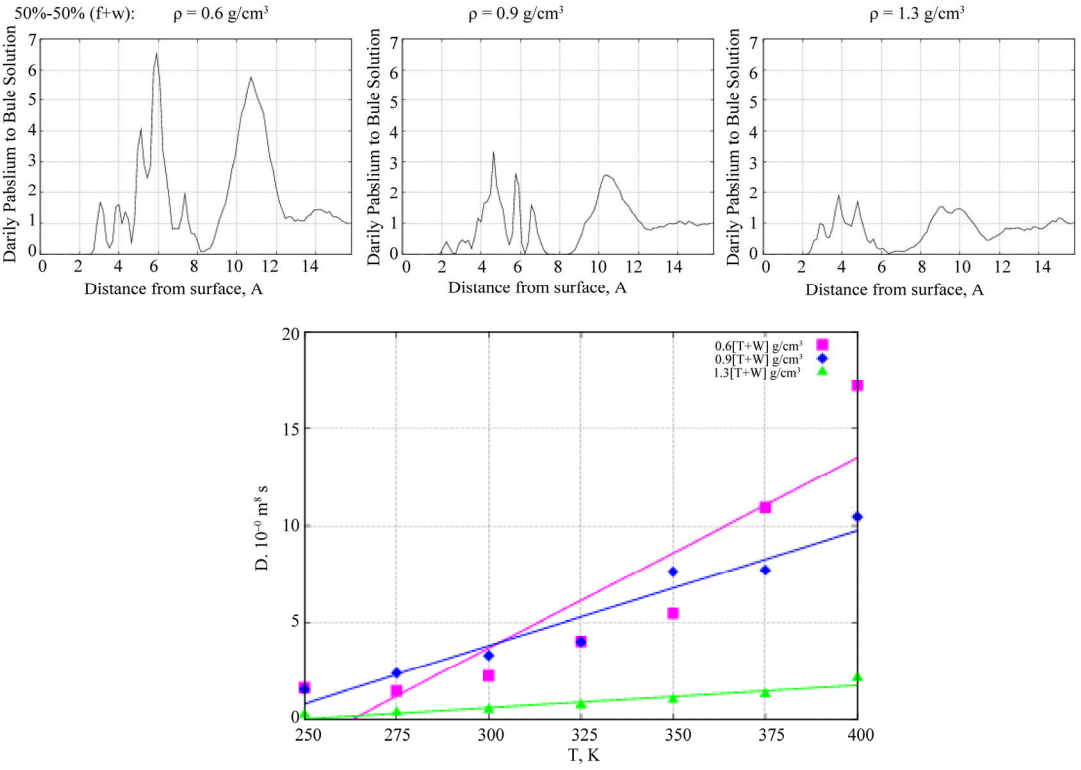

Figure 8. (top) The Z-density profiles of water molecules of 50% - 50% formamide-water solution as a function of perpendicular distance from the TiO_2 surface. (bottom) $D(T)$ behavior of the water molecules vs liquid density (pink—low, blue—moderate, green—high density phases).

essential modifications of the formamide diffusion ability on a TiO_2 surface in the presence of water. The bottom graph in **Figure 8** shows $D(T)$ curves for water—the diffusion coefficients depending on the system temperature. It is clear that with increasing the formamide-water concentration, the water diffusion coefficient decreases.

Next, **Figure 9** (top graphs) show the Z-density profiles of the formamide molecules on a TiO_2 surface in the presence of the 50% - 50% formamide-water (f + w) solution (left, middle, right: low, moderate, and high density phases, respectively). As seen from **Figure 9**, at low (left graph) and high (right graph) solution concentrations, the inclusion of water has no visible effect on the formamide density profile on the adsorbing surface. However, at moderate densities (middle graph, **Figure 9**), the formamide density distribution essentially changes normal to the surface. Namely, the two peaks of the Z-density profile that existed in the absence of water have been observed to disappear with the inclusion of water to the formamide-TiO_2 system, indicating an increase in the formamide diffusion ability. In **Figure 9** (bottom graph), the $D(T)$ dependences of formamide molecules are shown at different solution denstities in the presence of water. Comparing them to the ones in **Figure 6** (bottom graph) decribed above, one can easily see that at moderate solution densities water mediates $D(T)$ growth and thus causes an increase in the formamide diffusion abilities.

4. CONCLUSION

The effect of water inclusion on the formamide-titanium oxide (TiO_2) interaction mechanism has been studied via molecular dynamics (MD) simulation. The TiO_2 surface can act as a strongly adsorbing surface or a catalytic material. The aim of the present study was a comparative analysis of the formamide concentration distribution effects (the accumulation of molecules) on a TiO_2 surface in the absence and presence of a water solvent. The formamide diffusion ability on a TiO_2 surface is observed to correlate with the formamide-water concentration distribution on the surface. The structural radial distribution functions (RDFs) of water and formamide along with their Z-denstiy profiles point to crucial modifications

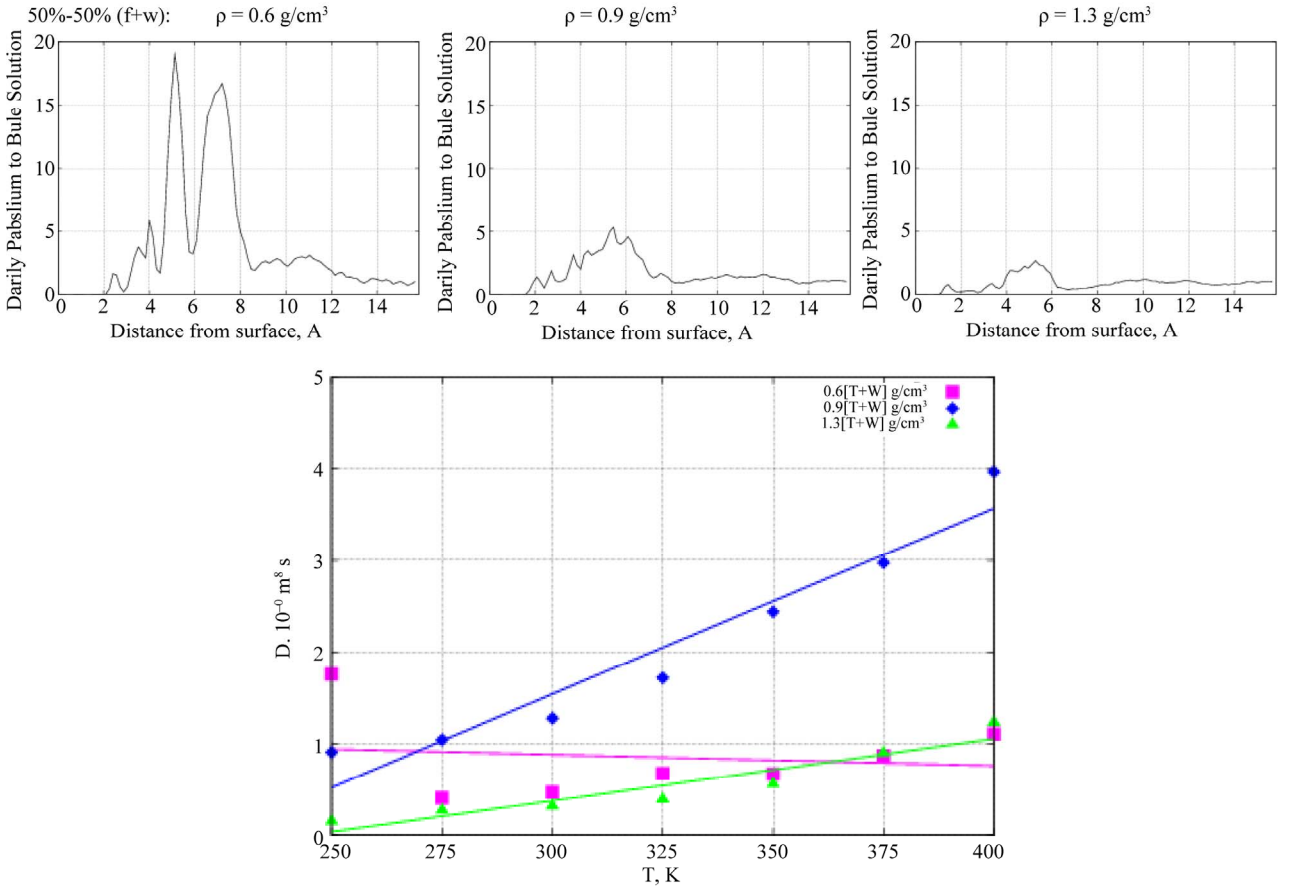

Figure 9. (top) The Z-density profiles of formamide molecules in the presence of water as a function of perpendicular distance from the TiO_2 surface. (bottom) $D(I)$ behavior of the formamide molecules vs liquid density (pink—low, blue—moderate, green—high density phases).

of the formamide diffusion ability on a TiO_2 surface mediated by the presence of water. The obtained results clear up the formamide-TiO_2 interaction mechanism on the molecular level and might be important for understanding the elementary steps of the formation of biological molecules needed for life.

5. ACKNOWLEDGEMENTS

This work has been performed as part of collaboration between JINR (Russia), RIKEN (Japan), and Keio University (Japan). The work has been supported in part by the Grant in Aid for the Global Center of Excellence Program to the Center for Education and Research of Symbiotic, Safe and Secure System Design from Japan's Ministry of Education, Culture, Sport, and Technology. The MD simulations have been performed using computer software, hardware facilities, and cluster machines at the CICC (JINR), RICC (RIKEN), and Yasuoka Laboratory of Keio University (Japan). The authors would like to specially thank Mr. Sergei Negovelov (JINR) for technical assistance and helpful comments.

REFERENCES

[1] Senanayake, S.D. and Idriss, H. (2006) Photocatalysis and the origin of life: Synthesis of nucleoside bases from formamide on TiO_2(001) single surfaces. *Proceedings of the National Academy of Sciences of the United States of America* (*PNAS*), **103**, 1194-1198. doi:10.1073/pnas.0505768103

[2] Saladino, R., Crestini, C., Costanzo, G. and DiMauro, E. (2004) Advances in the prebiotic synthesis of nucleic acids bases: Implications for the origin of life. *Current Organic Chemistry*, **8**, 1425-1443. doi:10.2174/1385272043369836

[3] Ferris, J.P., Hill, A.R. Jr., Liu, R. and Orgel, L.E. (1996) Synthesis of long prebiotic oligomers on mineral surfaces. *Nature*, **381**, 59-61. doi:10.1038/381059a0

[4] Ferris, J.P. (1993) Catalysis and prebiotic RNA synthesis. *Origins of Life and Evolution of Biospheres*, **23**, 307-315. doi:10.1007/BF01582081

[5] Huber, C. and Wächtershäuser, G. (1998) Peptides by activation of amino acids with co on (Ni,Fe)S surfaces: Implications for the origin of life. *Science*, **281**, 670-672. doi:10.1126/science.281.5377.670

[6] Kamineni, V.K., Lvov, Y.M. and Dobbins, T.A. (2007) Layer-by-layer nanoassembly of polyelectrolytes using formamide as the working medium. *Langmuir*, **23**, 7423-7427. doi:10.1021/la700465n

[7] Parmeter, J.E., Schwalke, U. and Weinberg, W.H. (1988) Interaction of formamide with the Ru(001) surface. *Journal of the American Chemical Society*, **110**, 53-62. doi:10.1021/ja00209a008

[8] Muir, J.M.R. and Idriss, H. (2009) Formamide reactions on rutile TiO_2(011) surface. *Surface Science*, **603**, 2986-2990. doi:10.1016/j.susc.2009.08.012

[9] Thiel, P.A. and Madey, T.E. (1987) The interaction of water with solid surfaces: Fundamental aspects. *Surface Science Reports*, **7**, 211-385. doi:10.1016/0167-5729(87)90001-X

[10] Henrich, V.E. (1985) The surfaces of metal oxides. *Reports on Progress in Physics*, **48**, 1481. doi:10.1088/0034-4885/48/11/001

[11] Henrich, V.E. (1979) Ultraviolet photoemission studies of molecular adsorption on oxide surfaces. *Progress in Surface Science*, **9**, 143-164. doi:10.1016/0079-6816(79)90011-X

[12] Henderson, M.A. (2002) The interaction of water with solid surfaces: Fundamental aspects revisited. *Surface Science Reports*, **46**, 1-308. doi:10.1016/S0167-5729(01)00020-6

[13] Diebold, U. (2003) The surface science of titanium dioxide. *Surface Science Reports*, **48**, 53-229. doi:10.1016/S0167-5729(02)00100-0

[14] Fujishima, A. and Honda, K. (1972) Electrochemical photolysis of water at a semiconductor electrode. *Nature*, **238**, 37-38. doi:10.1038/238037a0

[15] Schoffstall, A.M. and Laing, E.M. (1984) Equilibration of nucleotide derivatives in formamide. *Origins of Life and Evolution of Biospheres*, **14**, 221-228. doi:10.1007/BF00933661

[16] Schoffstall, A.M., Barto, R.J. and Ramos, D.L. (1982) Nucleoside and deoxynucleoside phosphorylation in formamide solutions. *Origins of Life and Evolution of Biospheres*, **12**, 143-151. doi:10.1007/BF00927141

[17] Berndt, A., Kosmehl, H., Celeda, D. and Katenkamp, D. (1996) Reduced formamide content and hybridization temperature results in increased non-radioactive mRNA *in situ* hybridization signals. *Acta Histochemica*, **98**, 79-87. doi:10.1016/S0065-1281(96)80053-5

[18] Chalmet, S. and Ruiz-López, M.F. (1999) Molecular dynamics simulation of formamide in water using density functional theory and classical potentials. *Journal of Chemical Physics*, **111**, 1117. doi:10.1063/1.479299

[19] Pomata, M.H.H., Laria, D., Skaf, M.S. and Elola, M.D. (2008) Molecular dynamics simulations of aot-water/formamide reverse micelles: Structural and dynamical properties. *Journal of Chemical Physics*, **129**, 244-503. doi:10.1063/1.3042275

[20] Smith, W., Forester, T.R. and Todorov, I.T. (2009) The DL POLY 2 user manual, version 2.20. STFC Daresbury Laboratory, Daresbury, Warrington WA4 4AD, Cheshire.

[21] Yong, C.W. (2010) DL Field—A force field and model development tool for DL POLY. In: Blake, R., Ed., *CSE Frontiers*, STFCs Computational Science and Engineering Department, 38-40.

[22] Brooks, B.R., Nilsson, L., *et al.* (2009) Charmm: The biomolecular simulation program. *Journal of Computational Chemistry*, **30**, 1545-1614. doi:10.1002/jcc.21287

[23] Kavathekar, R.S., Dev, P., English, N.J. and MacElroy, J.M.D. (2011) Molecular dynamics study of water in contact with the TiO_2 rutile-110, 100, 101, 001 and anatase-101, 001 surface. *Molecular Physics*, **109**, 1649-1656.

doi:10.1080/00268976.2011.582051

[24] Guillot, B. and Sator, N. (2007) A computer simulation study of natural silicate melts. Part I: Low pressure properties. *Geochimica et Cosmochimica Acta*, **71**, 1249-1265. doi:10.1016/j.gca.2006.11.015

[25] Matsui M. and Akaogi M. (1991) Molecular dynamics simulation of the structural and physical properties of the four polymorphs of TiO_2. *Molecular Simulation*, **6**, 239-244. doi:10.1080/08927029108022432

[26] Berendsen, H.J.C., Grigera, J.R. and Straatsma, T.P. (1987) The missing term in effective pair potentials. *Journal of Physical Chemistry*, **91**, 6269-6271. doi:10.1021/j100308a038

[27] Robinson, G.W., Singh, S., Zhu, S.-B. and Evans, M.W. (1996) Water in biology, chemistry and physics: Experimental overviews and computational methodologies. *World Scientific Series in Contemporary Chemical Physics*, **9**, 528.

[28] Kusalik, P.G. and Svishchev, I.M. (1994) The spatial structure in liquid water. *Science*, **265**, 1219-1221. doi:10.1126/science.265.5176.1219

[29] Mitchell, M.C., Gallo, M. and Nenoff, T.M. (2004) Computer simulations of adsorption and diffusion for binary mixtures of methane and hydrogen in titanosilicates. *Journal of Chemical Physics*, **121**, 1910-1916. doi:10.1063/1.1766019

[30] Chen, X. and Mao, S.S. (2007) Titanium dioxide nanomaterials: Synthesis, properties, modifications, and applications. *Chemical Reviews*, **107**, 2891-2959. doi:10.1021/cr0500535